

## Performance estimation and analysis of power line communication using single-ended loop testing

Bharathi MAYILSWAMY\*, Amsaveni AVINASHIAPPAN

Department of Electronics and Communication Engineering, Kumaraguru College of Technology, Coimbatore, India

Received: 05.12.2017

Accepted/Published Online: 03.04.2018

Final Version: 27.07.2018

**Abstract:** Using the electricity infrastructure for broadband data transmission is known as power line communication (PLC). The quality of broadband connectivity over a power line is a strong function of the line topology. Two-step hybrid single-ended loop testing (SELT) to estimate the open port loop topology of power lines is discussed in this paper. Correlation time domain reflectometry (CTDR) at different sockets is used to construct the initial topology. Optimization-based frequency domain reflectometry (FDR) is employed to ascertain more accurate power line topology. The discussed method has the advantage of reusing the existing DSL modem for the measurement and no prior knowledge is needed for the topology estimation. This method is validated for a wide range of line topologies with different numbers of bridge taps. The performance of the estimated topology is calculated using two-port network theory and the influence of the bridge taps on the performance of the line is analyzed.

**Key words:** Single-ended loop testing, correlation time domain reflectometry, frequency domain reflectometry, hybrid method, power line topology, capacity

### 1. Introduction

Digital subscriber line (DSL) is one of the widespread broadband technologies to deliver high data rates in the last feet applications using the existing copper infrastructure [1]. The recent variants of DSL technologies are very high speed digital subscriber line (VDSL2) and vectored VDSL (V-VDSL2). The operating frequency of both these technologies ranges up to 30 MHz [2,3] with a data rate of up to several hundred Mbps. The latest proposed and standardized DSL technology is G.fast [3,4], which aims to provide speeds exceeding 1 Gbps at a distance of 50 to 250 m over the copper twisted pair. G.fast is specified to operate up to 106 MHz [3,4]. Power line communication (PLC) is one of the attractive technologies in G.fast to support high speed home networking. The importance of PLC is mainly due to the readily available power line network and its high penetration rate. The feasibility of power lines for broadband data transmission is discussed in the literature [5].

The performance of the PLC mainly depends on the loop topology and the noise power spectral density (PSD) [6,7]. Power lines are different from telephone lines as they are built with thicker conductors (lesser gauge), are far shorter in length, and consist of higher number bridge taps (BTs). Further, the bridge taps are terminated with an assorted variety of impedances due to the varying nature of the electrical appliances connected. These appliances that are predominantly inductive result in time varying loads that are always

\*Correspondence: [bharathi.m.ece@kct.ac.in](mailto:bharathi.m.ece@kct.ac.in)

mismatched with the characteristic impedance of the transmission line [8,9]. It is importance to understand the line topology to analyze the performance of the system.

The G.hn and G.fast [2,4] facilitate the coexistence of DSL and PLC and as the frequency bands used in both these technologies overlap the issue of electromagnetic compatibility (EMC) arises. The effect of PLC interference on DSL mainly depends on the line topology [3,10]. Topology estimation plays an important role in analyzing the impact of PLC on DSL interference.

Topology estimation using single-ended loop testing (SELT) for two wire telephone lines is well studied in the literature [11–13]. A hybrid SELT method with a combination of correlation time domain reflectometry (CTDR) and frequency domain reflectometry (FDR) for the extraction of telephone line has been discussed [12,13].

Though the loop topology is an important parameter for attenuation modeling and the capacity calculation [7], the estimation of power line topology in the literature is very scarce. SELT developed for telephone lines cannot be directly used for power lines as the number of bridge taps in power lines is greater compared to telephone lines. In this paper, the extension of hybrid method is discussed using multipoint measurement and a procedure has been developed to construct the topology from the multipoint data. The effect of the bridge tap length and the location on the transfer function and capacity of the overall system is discussed.

Section 2 deals with topology estimation of power lines by multipoint hybrid method. Both CTDR and FDR methods are discussed. The application of this method for the power line topology estimation is discussed in Section 3. Section 4 discusses the effect of topology on the performance of the overall system. Concluding remarks are presented in Section 5.

## 2. Multipoint hybrid topology estimation

A multipoint CTDR-FDR method is discussed to estimate the power line network. Mathematical models of the echo signals in time domain and frequency domain developed for telephone lines [12,13] are applicable for power line networks as well. The basic line parameters of power lines are quite different from those of telephone lines as the thickness of the conductor is greater.

### 2.1. Primary line parameters

The transmission line can be characterized by the characteristic impedance and propagation constant, which is a function of the per unit line parameters given in Eqs. (1) to (4). The frequency dependent RLGC parameters are empirically obtained from [14] as follows:

$$R = \frac{2}{a} \sqrt{\frac{\mu f}{\pi \sigma}} (\Omega/m) \quad (1)$$

$$L = \frac{\mu}{\pi} \cosh^{-1} \frac{d}{a} + \frac{R}{2\pi f} (H/m) \quad (2)$$

$$C = \frac{\pi \varepsilon}{\cosh^{-1} \left( \frac{d}{a} \right)} (F/m) \quad (3)$$

$$G = 2\pi f C \tan \delta (S/m), \quad (4)$$

where

$a$ -diameter of the conductor in meters given by  $a = (0.127/1000) \times 92^{((36-n)/39)}$ ,  
 $n$ -gauge of the wire,  $d$ -distance between the conductors in meters,  
 $\mu$ -permeability of the medium in (H/m),  $\sigma$ -conductivity of the medium(S/m),  
 $\varepsilon$ -permittivity of the medium (F/m),  $\delta$ -skin depth in meters given by

$$\delta = \sqrt{1/(\pi f \mu \sigma)}$$

Power lines are 14 AWG lines and the values of the parameters are given in Table 1.

**Table 1.** Power line parameter values.

Parameters	Value
$d$	3.8 mm
$\mu$	$4\pi \times 10^{-7} H/m$
$\sigma$	$5.75 \times 10^7 S/m$
$\varepsilon$	$8.854 \times 10^{-12} F/m$

The propagation constant ( $\gamma$ ) and the characteristic impedance ( $Z_o$ ) are functions of the line parameters given by [15,16]

$$\gamma = \sqrt{(R + j\omega L)(G + j\omega C)} \quad (5)$$

At high frequencies  $R \ll \omega L$  and  $G$  is assumed to be zero. Under this condition the propagation constant is obtained by [15]

$$\gamma = \frac{R}{2} \sqrt{\frac{C}{L}} \left( 1 - \frac{R^2}{8\omega^2 L^2} \right) + j\omega \sqrt{LC} \left( 1 - \frac{R^2}{8\omega^2 L^2} \right) \quad (6)$$

$$Z_o = \sqrt{\frac{R + j\omega L}{G + j\omega C}} \quad (7)$$

These characteristic properties of the power line are used to model the time domain and frequency domain echoes using the model developed in [12].

## 2.2. Multipoint CTDR method

The PLC network typically consists of a large number (more than 5) of bridge taps. The echo signal in time domain is expressed as [12]

$$r(t) = \sum_{i=1}^M e_r^{(i)}(t - T_i) + N_0(t), \quad (8)$$

where  $M$ -number of discontinuities in the line,

$N_0(t)$ -noise present in the channel,  $T_i$  - time of arrival of the  $i$ th echo

$e_r^{(i)}(t)$ -echo generated by the  $i$ th discontinuity.

It is observed that the received echo is more influenced by the first few bridge taps and the effect of the remaining bridge taps is minimal [12]. At each bridge tap discontinuity, the transmitted signal strength

is reduced to  $\sim 30\%$  (transmission coefficient of bridge tap  $\sim -0.3$ ) of incident value. This reduction, when cumulated, results in too weak an echo signal from far end discontinuities. For example, reflection from the 2nd discontinuity is  $\sim 2.7\%$  ( $0.33 \times 0.33 \times 0.33$ ) of the input signal, considering the signal loss only due to the discontinuity and hence becomes insensitive beyond the 3rd tap. Due to this reason, the CTDR SELT technique using a single point measurement is not capable of complete topology estimation. A de-embedding technique as presented in [12] for telephone lines is also found to be limited in handling high numbers of bridge taps. A multipoint measurement is used to overcome this limitation [8]. In the multipoint method, TDR measurement from each socket is analyzed to predict the finite segments close to the measuring socket.

The predicted line segments accuracy is improved by Nelder–Mead optimization algorithm [17] by comparing the simulated echo of the predicted loop with the received echo in the localized time period. Applicability of the iterative method for the complete network is tedious for PLC, as it often converges to local minima due to the high number of variables (number of variables =  $2 \times$  no of taps + 1). To overcome this limitation, fine tuning of the line length is performed at the line segment level and not at the complete topology level. Identified line segments close to each socket are used to construct the complete topology ( $\Phi$ ).

The steps for constructing the complete topology are given below.

1. Correlated signal at the start point will have multiple pairs of peaks (from junction and the end of bridge tap).
2. Correlated signal at the intermediate sockets will have a single peak (due to the bridge joint to the main line) followed by pairs of peaks.
3. Correlated signal at the end of the loop will have an additional single peak due to the end of loop in addition to the characteristics of intermediate sockets.
4. At the start point (P1), identified bridge taps are in sequence.
5. At the last socket the end of loop is identified from the reflection coefficient. Reflection from the end of loop will be much higher amplitude as the reflection coefficient of the open end (1) is higher than that of the bridge tap (0.33).
6. For the rest of the points (P2 to P5), estimated segments lengths are verified with the start point and end point predictions to finalize the immediate next segments.

The FDR verification step for the complete topology from the multipoint CTDR is presented in the next section.

### 2.3. FDR verification

Predicted loop topology is validated by means of the FDR method at multiple sockets. Predicted loop  $\Phi$  is used to generate the FDR data  $R(\Phi, f_n)$  using Eq. (9):

$$R(f_n) = \sum_{i=1}^M \left( R^{(i)}(f_n) + N_o(f_n) \right) \quad (9)$$

This is compared with the measured FDR data ( $\hat{R}(f_n)$ ) in terms of mean square error (MSE) value as shown in Eq. (10):

$$MSE = \left( \sum_{n=1}^N |R(\Phi, f_n) - \hat{R}(f_n)|^2 \right) \tag{10}$$

Figure 1 gives the flow chart for the combined multipoint CTDR and FDR method. The applicability of the developed method for the topology identification is given in the next section.

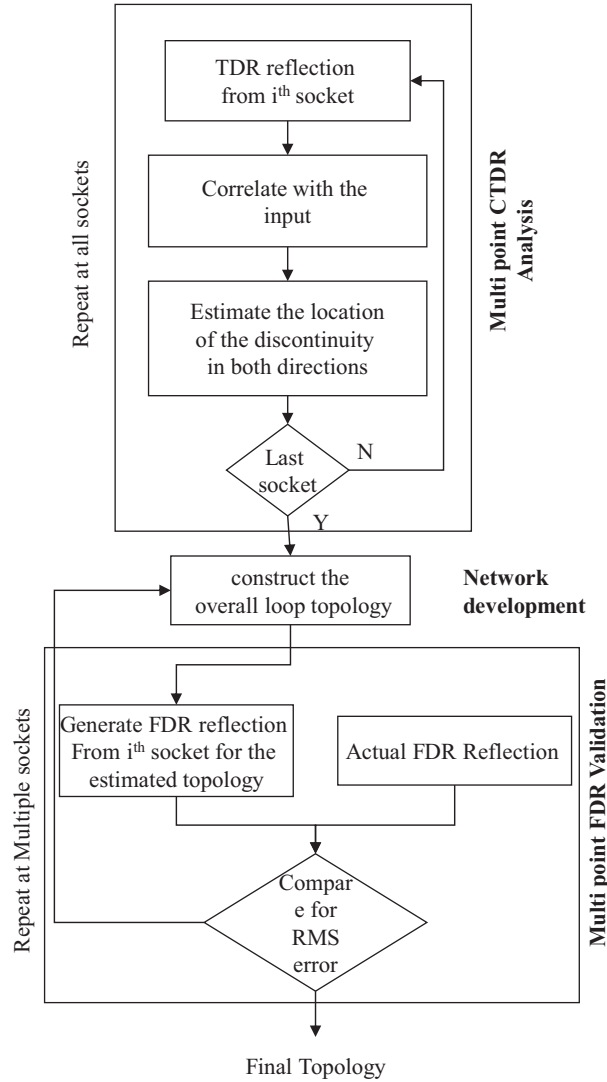


Figure 1. Multipoint CTDR-FDR method.

### 3. Result of topology estimation

The test loops considered for the verification of the developed method are shown in Figure 2 with line segment lengths indicated in meters. Test loop 1 is a plain line and loops 2, 3, and 4 are used to test single bridge tap with change in location and tap length. Test loops 5, 6, and 7 are defined with 2, 5, and 10 taps, respectively.

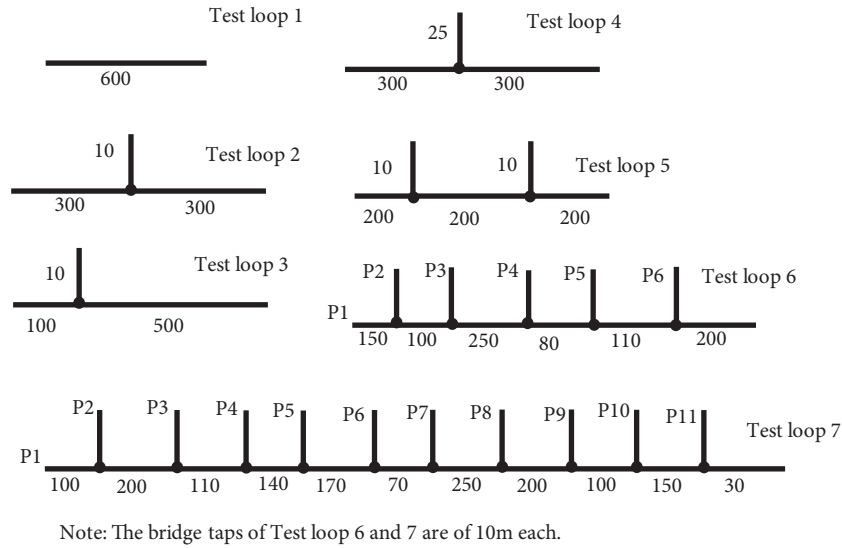


Figure 2. Test loops.

The single point CTDR and FDR method is capable of predicting the topology for test loops 1 to 5 that have one or two bridge taps. The waveforms and the analysis of single point CTDR and FDR are explained with test loop 2, which is a loop with one bridge tap. For this loop, the variation of correlation amplitude with reach is shown in Figure 3. As power lines will have only bridge tap-type discontinuities, the magnitude of the correlated signal is plotted without considering its sign. From Figure 3, the following line characteristics are deduced.

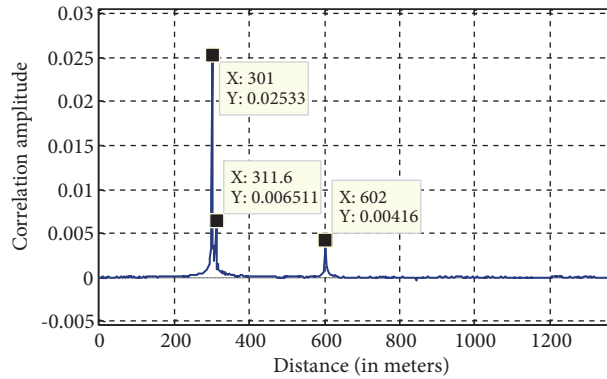


Figure 3. Correlation amplitude vs. distance for test loop 2.

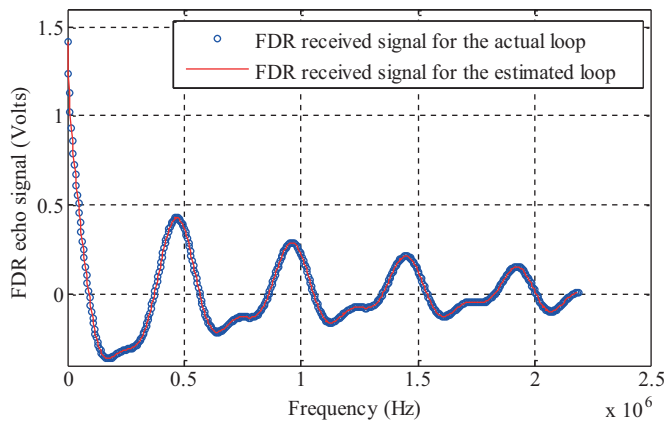
1. Bridge tap is present as there is more than one peak.
2. Peaks at 311.6 m and 301 m indicate the tap length of 10.6 m (311.6–301) at 301 m.
3. Second line segment is 301 m (602 m–301 m).

The location and the length of the bridge taps are fine-tuned by the optimization method. The initial and final estimated topologies are shown in Table 2. The FDR-based validation is shown in Figure 4 with the mean square error of 0.0017.

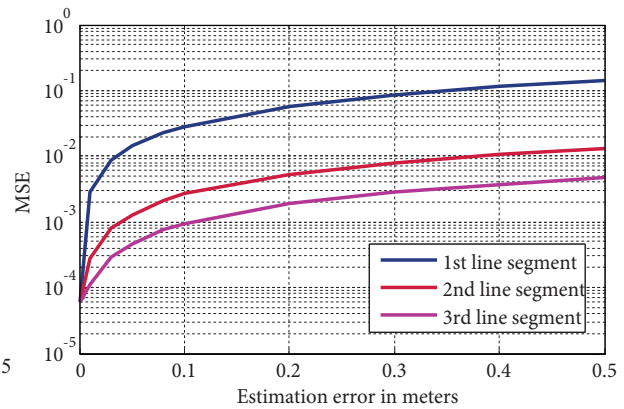
**Table 2.** Estimated topology for test loop 2.

Initial estimated topology (in meters)	Final estimated topology (in meters)
 ⊗ -indicates the measurement point	

The validation of topology using FDR largely depends on the error in the estimation of the first segment length, whereas the errors in the 2nd and 3rd segment lengths have less contribution to the mean square error. Figure 5 shows the effect of the error in segment lengths on the MSE value. It is observed that for a line with multiple segments MSE is one order higher if the error is in the first segment compared to that in the second or third segments from the measuring socket. This confirms that echo-based topology estimation methods are not effective for higher numbers of discontinuities. To overcome this limitation a multipoint SELT technique is developed and verified for test loops 6 and 7.



**Figure 4.** FDR validation for test loop 2.



**Figure 5.** MSE variation due to estimation error.

For PLC test loop 7, the correlated amplitude variation with distance from points P1 to P11 are shown in Figure 6a and 6b. The initial and final predicted loop topology from each measuring socket is tabulated in Table 3.

As the number of bridge taps is more FDR validation is carried out from multiple points. The simulated FDR with the predicted topology and the FDR of the actual loop is shown in Figure 7. The predicted topology for test loop 7 is shown in Figure 8.

The above results proved that the use of multipoint CTDR is capable of predicting the loop topology with multiple bridge taps. The estimation error is less than 1% in terms of line lengths for all the test loops defined. With repeated trials, the variance in the estimation was found to be much less (<4%). The effect of bridge taps on the transfer function and the performance is discussed in the next section.

#### 4. Performance estimation

The transfer function of the loop is derived using the cascaded transmission matrix method [15,16]. Transmission matrix of a line segment, bridge tap, and that of the network are given in Eqs. (11)–(14). The R, L, C, G

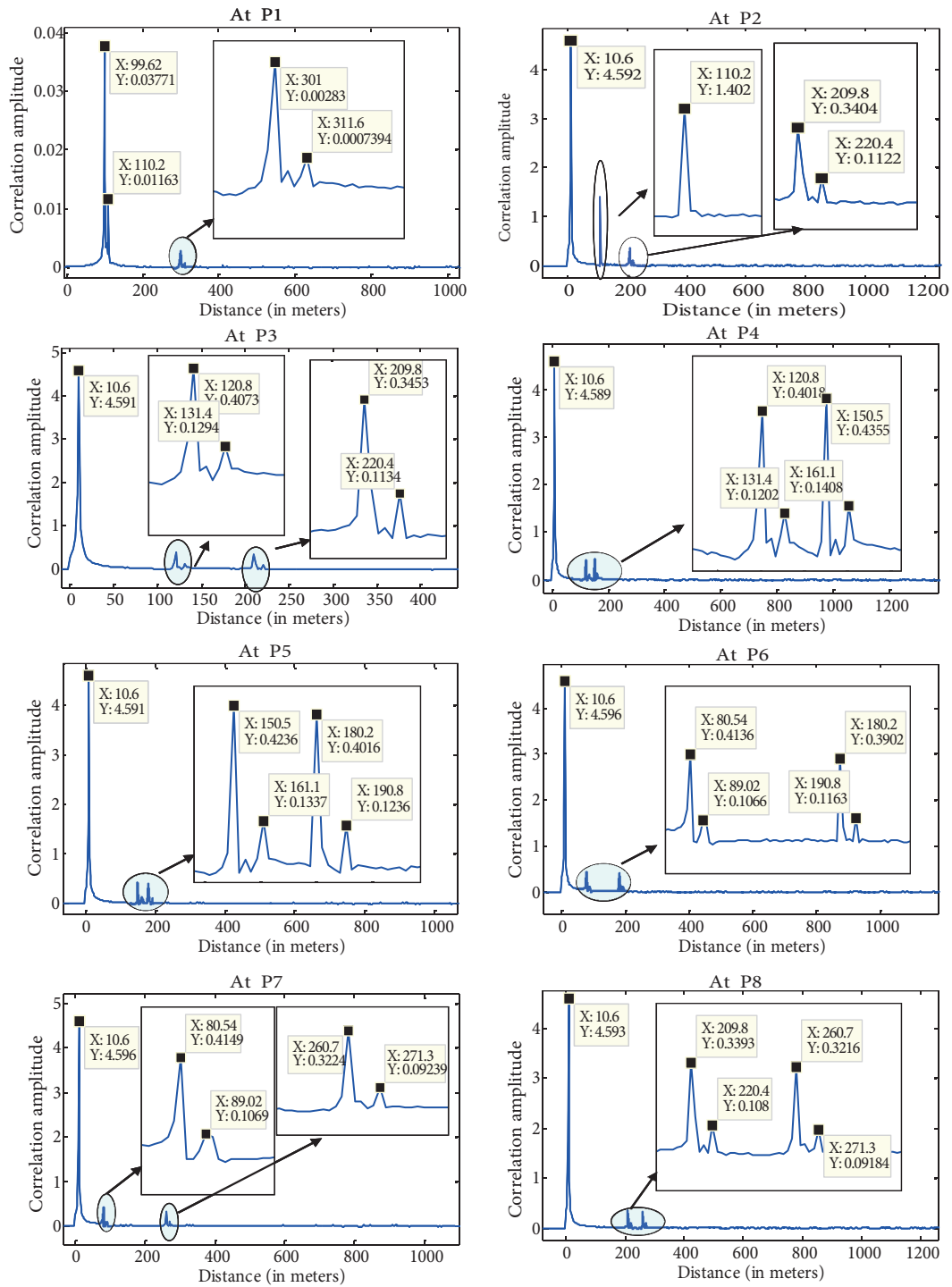


Figure 6. (a). Correlated signal at points P1–P8 for test loop 7.



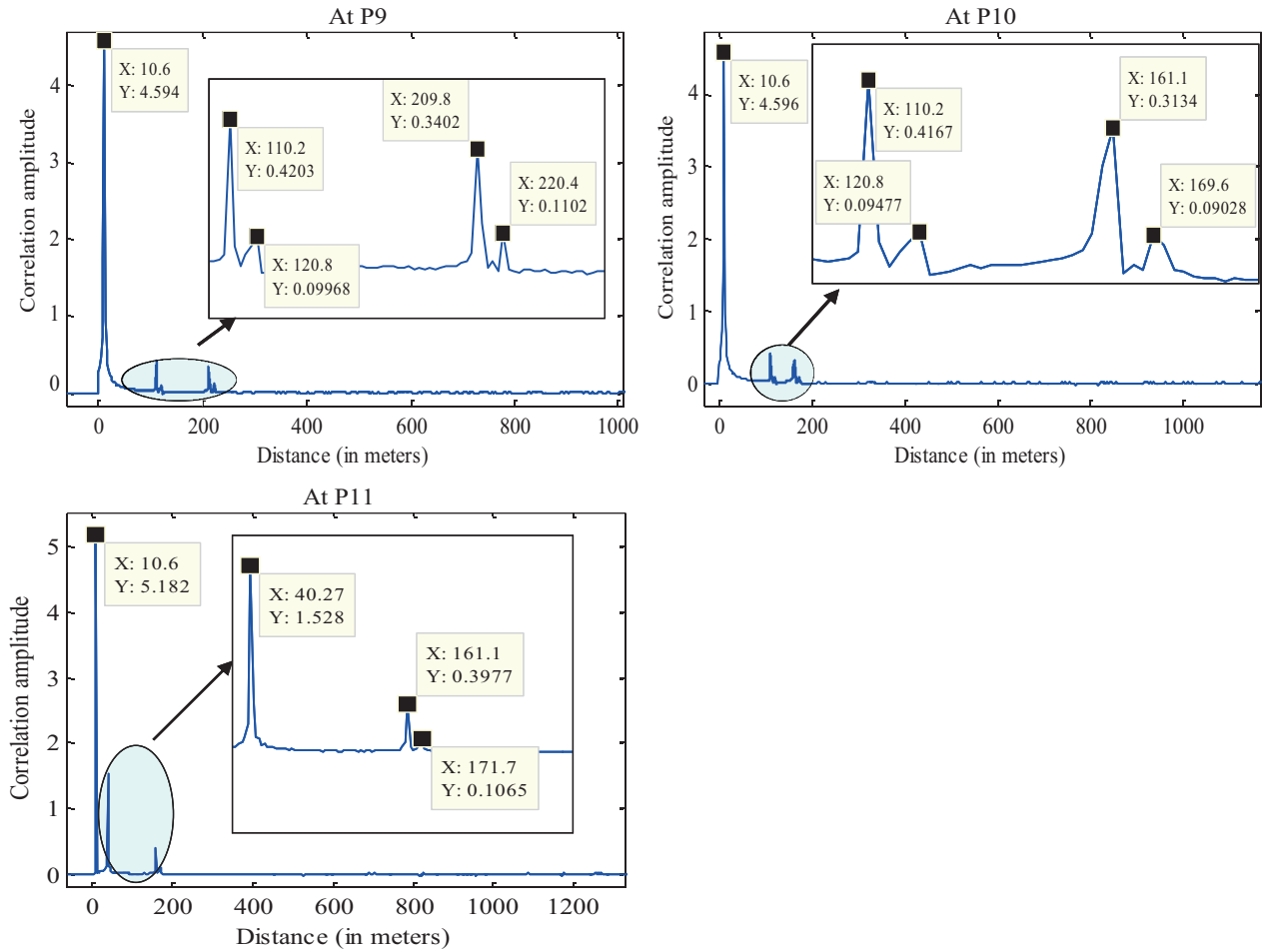


Figure 6. (b). Correlated signal at points P9–P11 for test loop 7.

parameters and the propagation constant discussed in section 2 are used for this calculation.

$$T = \begin{bmatrix} A & B \\ C & D \end{bmatrix} = \begin{bmatrix} \cosh(\gamma L) & Z_o \sinh(\gamma L) \\ \frac{\sinh(\gamma L)}{Z_o} & \cosh(\gamma L) \end{bmatrix} \quad (11)$$


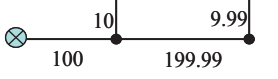


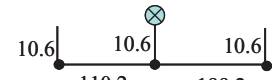
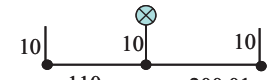
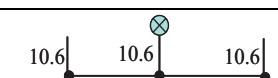
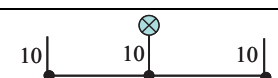
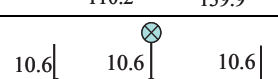
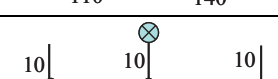
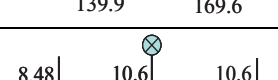
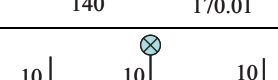
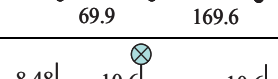
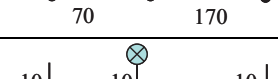
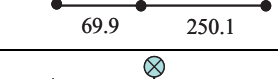
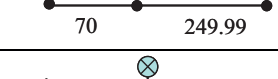
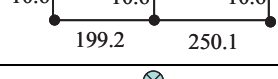
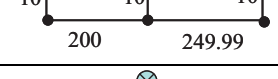
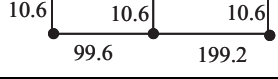
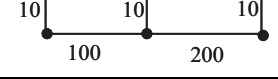
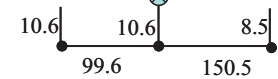
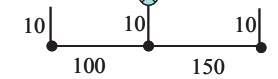
$$T_{tap} = ABCD_{tap} = \begin{bmatrix} 1 & 0 \\ \frac{1}{Z_{0,tap} \coth(\gamma L_{tap})} & 1 \end{bmatrix} \quad (12)$$

$$T = \begin{bmatrix} A & B \\ C & D \end{bmatrix} = T_1 \times T_2 \times \dots \times T_N = \prod_{i=1}^N \begin{bmatrix} A_i & B_i \\ C_i & D_i \end{bmatrix} \quad (13)$$

$$H(f) = \frac{Z_L}{AZ_L + B} \quad (14)$$

Tests are conducted to quantify the effect of a discontinuity in a loop. Presence of a bridge tap results in a steep dip (null) in the transfer function at a specific frequency [18]. The characteristics of the nulls depend on the

**Table 3.** The estimated line segments from points P1-P11 for test loop 7.

Point	Initial estimated topology (in meters)	Final estimated topology (in meters)
P1		
P2		
P3		
P4		
P5		
P6		
P7		
P8		
P9		
P10		
P11		

length of the tap ( $d$ ). The transmitted signal travels through the tap for a distance of  $2d$  and combines with the main loop signal. The phase at which it joins the main loop signal determines its effect on the transfer function. For example, if  $d = \lambda/4$ , the signal propagates a distance of  $\lambda/2$  and will be out of phase with the main loop signal. This results in a reduction in main loop signal amplitude by the amplitude of the return signal from the tap, which creates nulls in the transfer function. Amplitude of the null is a strong function of tap length. For

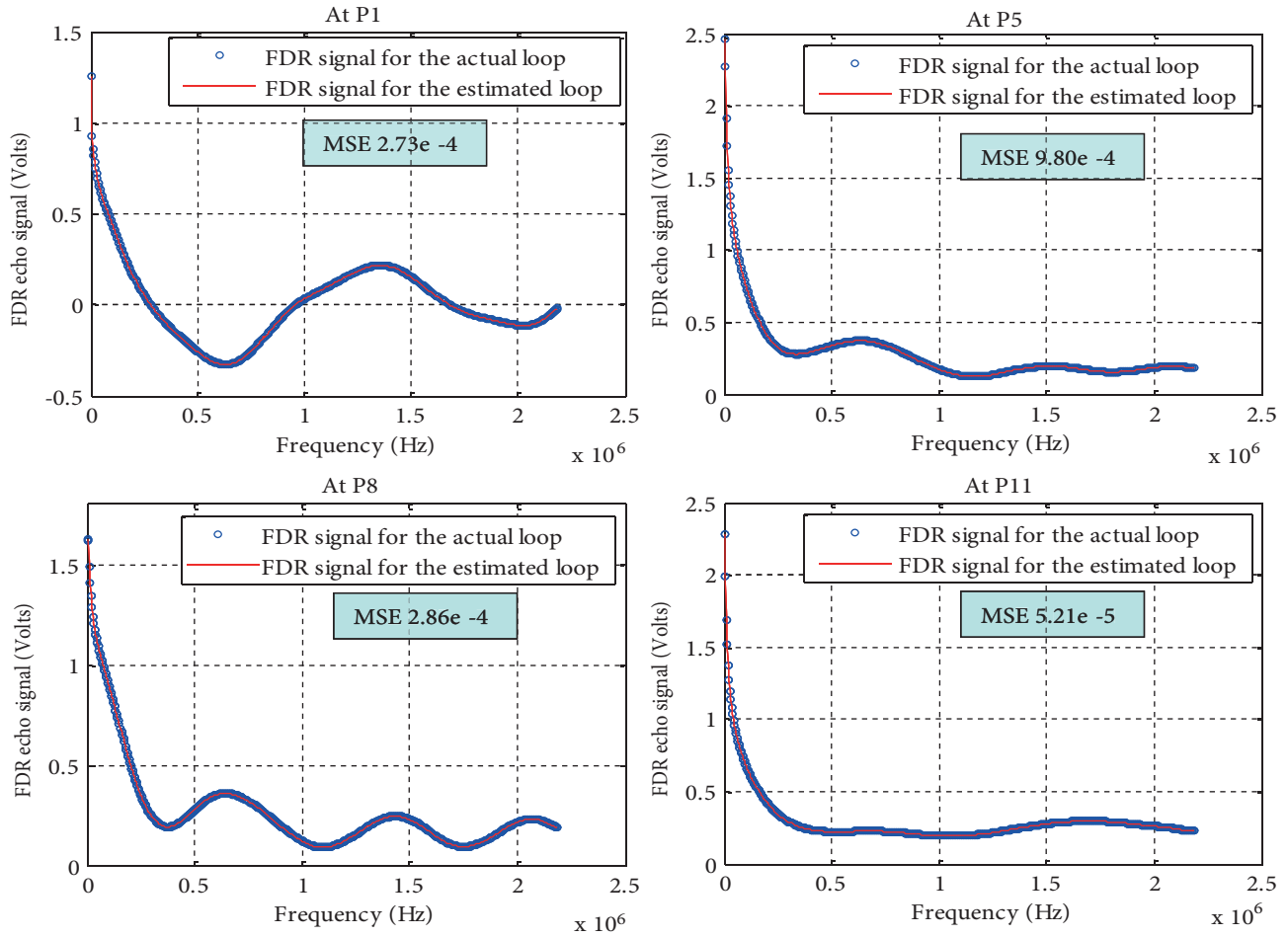


Figure 7. FDR validation for test loop 7.

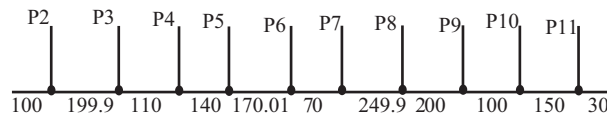


Figure 8. Predicted topology for test loop 7.

smaller length taps, the attenuation of the signal through the tap is minimal and results in a deeper null. Thus a smaller bridge tap is more damaging than longer ones as it introduces more propagation loss. The frequency at which the null occurs is also a function of the tap length. The first null occurs at  $f_N = V/(4 \times d)$ .  $V$  is the velocity of propagation. This repeats for the odd multiples of  $f_N$ .

Test loops 1–5 are defined with a constant total length of 600 m and their transfer function is plotted in Figure 9. As there are no bridge taps in loop 1, the transfer function is gradually reducing. Sudden dips in the transfer function are observed for loops with bridge taps. As discussed earlier, a sharp reduction (dip) in the transfer function is observed at a frequency of  $V/4d$  for every bridge tap of ‘ $d$ ’ meters length. This dip repeats for odd multiples of the calculated frequency.

For test loops 2 and 3, the transfer function is almost identical with a dip at 7.4 MHz even though

the position of the bridge tap is different. From this observation it is concluded that the transfer function is independent of the location of the bridge tap but depends only on the length of the tap. The location of the dip in transfer function for loop 5 remains at 7.4 MHz as the length of the taps is 10 m. However, the depth of the null in loop 5 is more due to the higher number of taps. With 25 m tap length, loop 4 has a dip at 2.9 MHz and at its odd multiples. As the tap length in this case is higher, the depth of the null is shallow.

The transfer function of test loops 6 and 7 is shown in Figure 10. The depth of null in test loop 6 is higher ( $-180$  dBm) compared to loops 2–5 due to the increased number of bridge taps. The magnitude of the nulls in test loop 7 is twice that of loop 6 as the number of bridge taps is doubled.

Maximum data rates for the estimated topologies are computed with the transfer function and noise PSD. In power lines AWGN noise and impulse noise are the dominant sources in power lines. In the present capacity calculation, AWGN is considered. The impedance of an electrical appliance is generally complex. As a typical electrical appliance is inductive in nature (60 mH), its impedance is much higher compared to the characteristic impedance of the line in the usable frequency range. Hence considering bridge tap as an open termination in the transfer function calculation is a valid approximation. As there is no standard on the limit of power spectral density (PSD mask) defined for power lines, in our capacity calculation, the PSD mask of all digital mode in VDSL 2 is used as this helps in comparing the data rate efficiency of power lines with VDSL. The band plan of VDSL 2 [19,20] is considered for the capacity calculation. The downstream capacity of the test loops is tabulated in Table 4.

**Table 4.** Downstream capacity for test loops.

Test loop	Downstream data rate (Mbps)
test loop 1	192.02
test loop 2	150.71
test loop 3	150.50
test loop 4	152.70
test loop 5	138.78
test loop 6	112.04
test loop 7	89.06

The channel capacity is a function of the length of the line, the number of taps, and the length of the tap. Figure 11 shows the variation of downstream capacity as a function of number of taps (10 m tap length) and tap length for a 600 m line. The channel capacity increases with tap length. However, beyond 15 m tap length the capacity remains almost constant. The capacity of the line reduces exponentially with an increase in the number of taps and about 80% of the reduction the capacity is observed for the first 10 taps.

## 5. Conclusion

Topology estimation methods developed for telephone lines are not directly applicable to power lines due to shorter line lengths, change in gauge, and significantly higher number of bridge taps. To overcome these challenges, a new multipoint CTDR-based SELT method is presented for power line topology estimation. In this method, finite line segments close to each socket are identified by multipoint measurement and used to construct the complete topology. An algorithm to build the complete network from the individual segments is developed in MATLAB. Multipoint FDR data are used to validate the constructed topology for test loops.

For the identified loops, the transfer function is calculated based on the transmission matrix. It is found that the presence of bridge taps results in a dip in the transfer function at frequencies  $V_{oP}/4d$  and at its odd multiples. The frequency and depth of dip are a strong function of the tap lengths and the location of the tap has no influence on the transfer function. This proposed model is tested for loops with a maximum of 10 taps and with varying tap lengths. Finally, capacity of the loop is calculated using the PSD mask of all digital modes of VDSL 2. With AWGN noise, the capacity was found to be in the order 100 Mbps for test loops with lower number of taps ( $<5$ ) and 89 Mbps for test loop with 10 taps. Further, to improve the applicability of this method for real time topology estimation and capacity calculation, impulse noise shall also be included along with AWGN.

### References

- [1] Khan A, Baig S, Nawaz T. DWMT transceiver equalization using overlap FDE for downlink ADSL. Turk J Elec Eng & Comp Sci 2015; 23: 681-697.
- [2] ITU (International Telecommunication Union). Unified high-speed wireline-based home networking transceivers – Multiple input/multiple output specification, Std. G.9963; 2011.
- [3] Kerpez K, Galli S, Mariotte H, Moulin M. The impact of PLC-to-DSL interference on VDSL2, vectored VDSL2, and G.fast. In: IEEE 2015 International Symposium on Power Line Communication; 29 March–1 April 2015; Austin, TX, USA.
- [4] ITU (International Telecommunication Union). Fast access to subscriber terminals (G.Fast) –Physical layer specification, Std. G.9701; 2014.
- [5] Galli S, Logvinov O. Recent developments in the standardization of power line communications within the IEEE. IEEE Commun Mag 2008; 46: 64-71.
- [6] Oksman, Galli S. G.Hn: the new ITU-T home networking standard. IEEE Commun Mag 2008; 47: 138-145.
- [7] Meng H, Chen S, Guan YL, Law CL, So PL, Gunawan E, Lie TT. Modeling of transfer characteristics for the broadband power line communication channel. IEEE T Power Deliver 2004; 19: 1057-1064.
- [8] Ravishankar S, Bharathi M. Line topology estimation of indoor power lines using multipoint single ended loop testing. International Journal of Future Generation Communication and Networking 2012; 5: 55-71.
- [9] Ravishankar S, Arjun R. A hybrid method for physical and power line loop topology estimation using a broadband modem. In: IEEE Symposium on Radio and Wireless Symposium 2016; 24–27 January 2016: Austin, TX, USA.
- [10] Ali K, Messier G, Lai S. DSL and PLC co-existence: an interference cancellation approach. IEEE T Commun 2014; 62: 3336-3350.
- [11] Lima VD, Klautau A, Costa J, Ericson K, Fertner A, Sales C. A wavelet-based expert system for digital subscriber line topology identification. Int J Commun Syst 2014; 29: 47-63.
- [12] Bharathi M, Ravishankar S. Single ended loop topology estimation using FDR and correlation TDR in a DSL modem. Cyber Journals: Multidisciplinary Journals in Science and Technology, Journal of Selected Areas in Telecommunications 2012; 40-48.
- [13] Ravishankar A, Ravishankar S. Extraction of two wire and power line loop topology using customized genetic algorithms. In: Sixth International Symposium on Embedded Computing and System Design 2016; 15–17 December 2016: Patna, India.
- [14] Li H, Sun Y, Yao Y. The indoor power line channel model based on two-port network theory. In: International Conference on Signal Processing 2008; 26–29 October Beijing, China: 132-135.
- [15] Ryder JD. Networks, Lines and Fields. 2nd ed. Upper Saddle River, NJ, USA: Prentice Hall, 1978.

- [16] Starr T, Cioffi JM, Silverman PJ. Understanding Digital Subscriber Line Technology. New York, NY, USA: Prentice Hall, 1999.
- [17] Luersen MA, Le R, Guyon F. A constrained, globalized, and bounded Nelder–Mead method for engineering optimization. *Struct Multidiscip O* 2004; 27: 43-54.
- [18] Im G. Performance of a 51.84-Mb/s VDSL transceiver over the loop with bridged taps. *IEEE T Commun* 2002; 50: 711-717.
- [19] ITU (International Telecommunication Sector). Very high speed digital subscriber line transceivers 2 (VDSL 2); 2006.
- [20] Sharma S, Om PS. A dynamic spectrum management algorithm in VDSL systems. *Turk J Elec Eng & Comp Sci* 2016; 24: 3483-3491.